Chapter 7

Repair of DNA double strand breaks caused by piggyBac transposition

7.1 Introduction

One of the most striking properties of the piggyBac transposon (PB) is its precise excision from the genome (Ding *et al.*, 2005). In mouse ES cells, 95% of excision events were found to be precise (Wang *et al.*, 2008). This is unusual for a transposable element and has led to investigation of a novel use for PB—removal of transgenes from a genome. Two studies have used PB to introduce reprogramming transgenes for the creation of induced pluripotent stem cells (iPS cells, Yusa *et al.* (2009); Woltjen *et al.* (2009)). In these studies, the transposon is remobilised in the resulting iPS cells and subclones isolated where the transposon has not reintegrated. Due to the precise repair of the donor site, these cells are proposed to have a 'clean' genome, and thus are potentially suitable for therapeutic use, e.g. transplantation. In a related application, currently being pursued in our laboratory, PB can be used as an alternative to Cre-loxP or Flp-FRT recombinase systems for removal of selectable markers after gene targeting. Using site-specific recombinases for this purpose always leaves a single copy of the target site after removal. This is not optimal, as it is difficult to be sure that the remaining target site does not disrupt a functional element in some way. Furthermore, in extensively engineered cells or mice there may be many copies of the site in the genome, which could potentially recombine to cause inversions, translocations or deletions. In contrast, using PB to remove a selectable marker after targeting will leave no other mutation at the locus, provided that the PB is engineered into an endogenous TTAA site.

If such methods are to be used clinically, it is important to understand them thoroughly. Very little is known about the biochemistry of PB excision, essentially all coming from one published study (Mitra *et al.*, 2008). Repair of the donor site was not addressed in this study. In this chapter I describe the use of the *Hprt-PB* reporter locus developed for library generation to study repair of the break produced by PB excision. I found a genetic requirement for the nonhomologous end joining (NHEJ) factors *Xrcc4* and *Xlf* in accurate repair. The tools that I have developed constitute a new method to program and study the repair of double strand breaks in mammalian cells.

7.1.1 Excision of transposons

There are several known families of transposons with different mechanisms of excision. Transposases such as SB cleave both strands of DNA, usually at staggered positions, and thus cause a double strand break. The structure of the end produced depends on the exact position of cleavage and the ends are not necessarily compatible—SBase produces a three nucleotide non-complementary 3′ overhang (Luo *et al.*, 1998).

Other transposases make a single stranded nick, exposing a 3′ hydroxyl group, which is then used to break the second strand by nucleophilic attack. This produces terminal hairpins at the site of attack, which must be processed before the site is repaired. PB is an example of this category, which also includes the RAG1/RAG2 recombinase—a domesticated transposase used in V(D)J recombination in lymphocyte development.

An *in vitro* study using purified recombinant PBase and a minimal PB element has characterised the mechanism of PB excision and integration (Mitra *et al.*, 2008). PB leaves four nucleotide 5′ overhangs, and these are compatible as the PB insertion site (TTAA) is four bp in length and duplicated upon insertion. The two ends should, therefore be directly ligatable. Several host double strand break repair pathways could potentially handle this type of break, discussed below.

7.1.2 Cellular double strand break repair pathways

A single unrepaired double strand break (DSB) is a lethal lesion (Bennett *et al.*, 1993) because of signalling events that stall cell cycle progression and eventually cause apoptosis in response to DNA damage. This DNA damage response (DDR) is tailored

to the cell cycle phase and type of damage occurring (Jackson, 2002). In mammalian cells, the two major pathways of double strand break repair are nonhomologous end joining (NHEJ) and homologous recombination (HR; Figure 7.1).

Nonhomologous end joining

NHEJ, as the name implies, joins free DNA ends together without the use of sequence homology to guide pairing. In this sense, it can be considered an error-prone pathway, as two ends that do not belong together could be joined. NHEJ can also introduce mutations at the break point if the ends are processed before joining. This processing may involve removal or addition of nucleotides.

Nonhomologous end joining is used much more widely in mammalian cells compared to yeast, and many of the essential proteins were identified in mammalian systems, by a combination of biochemistry and complementation analysis of X-ray sensitive Chinese hamster ovary (CHO) cells (Jeggo and Kemp, 1983). T and B lymphocyte development relies on NHEJ for repair of developmentally programmed breaks in V(D)J recombination and class switch recombination, two processes that generate diversity at the immunoglobulin and T-cell receptor (TCR) loci (Dudley *et al.*, 2005). Therefore, lymphocyte developmental defects have also been useful for the study of NHEJ. The first factor involved is the heterodimeric Ku protein complex, which binds tightly to free DNA ends (Mimori *et al.*, 1986). These proteins form part of the DNA-dependent protein kinase (DNA-PK), which is completed by binding of the third component, the catalytic subunit DNA-PKcs (Gottlieb and Jackson, 1993).

Mutations in the *Prkdc* gene, which encodes DNA-PKcs, were found to be responsible for the phenotype of severe combined immunodeficiency (SCID) mice (Blunt *et al.*, 1995, 1996). SCID mice, as well as mice with targeted mutations in *Prkdc* are defective in T and B lymphocyte development (Gao *et al.*, 1998; Taccioli *et al.*, 1998). More specifically, such mice are deficient in processing and joining coding ends in V(D)J recombination—the process by which different segments of the immunoglobulin genes are juxtaposed to generate TCR and antibody diversity. This involves resolution of a hairpin intermediate, much like that generated at the ends of the excised PB transposon. In contrast, the blunt signal ends of the excised sequence in the V(D)J recombination process are repaired normally in SCID and $Prkdc^{-/-}$ mice. Targeted knockouts of either of the two Ku subunits also lead to immunodeficiency; however in this case both coding and signal joins are affected (Nussenzweig *et al.*, 1996; Gu *et al.*, 1997a,b; Zhu *et al.*, 1996).

DNA-PK regulates the ongoing DNA damage response by activating itself by autophosphorylation in *trans*, and also by phosphorylating other proteins required for end processing. Many physiological DNA breaks will contain complex structures that can not be ligated, so require processing by nucleases and polymerases. Several enzymes that process ends are known, including the Artemis nuclease (which forms a complex with DNA-PKcs), terminal deoxynucleotidyl transferase (TdT) and the polymerases μ and λ. *Artemis* knockout mice have a similar phenotype to *Prkdc* knockouts, supporting an essential role in repair of ends that require processing prior to ligation (Rooney *et al.*, 2003).

Another important kinase in the signalling response to DNA damage is ATM (Ataxia Telangiectasia Mutated). ATM is activated in response to very low levels of DNA damage, corresponding to just a few breaks per cell (Bakkenist and Kastan, 2003) and phosphorylates a number of cell cycle regulators and DNA repair proteins (Shiloh, 2003). Although ATM is not directly involved in repair of DSBs, cells from ataxia telangiectasia (AT) patients are radiosensitive, as are *Atm*-deficient ES cells (Xu and Baltimore, 1996). A subset of DSBs caused by IR persists in ATM-deficient cells and cells treated with an ATM inhibitor. This set of ATM-dependent DSBs may represent breaks occurring in heterochromatin or breaks with complex structures (Goodarzi *et al.*, 2008).

The ligation itself in NHEJ is carried out by DNA Ligase IV. Although DNA Ligase IV is sufficient for the ligation of certain substrates *in vitro*, in cells it forms a complex with the XRCC4 protein. In the absence of XRCC4, DNA Ligase IV protein is destabilised and its ligation activity reduced (Grawunder *et al.*, 1997; Bryans *et al.*, 1999). The two proteins are thus functionally linked. More recently, a new component of the ligation complex was identified: XRCC4-like factor (XLF, also known as Cernunnos. Ahnesorg *et al.* (2006); Buck *et al.* (2006)). Purified XLF stimulates the activity of XRCC4-DNA Ligase IV in *in vitro* assays. XLF can be considered a core NHEJ component, as XLF-deficient cells display increased radiosensitivity (Ahnesorg *et al.*, 2006).

In contrast to the early-acting NHEJ factors, knocking out *Xrcc4* or *Lig4* in mice results in embryonic lethality (Frank *et al.*, 1998; Gao *et al.*, 1998; Zha *et al.*, 2007). There appears to be a particular requirement for these factors in the de-

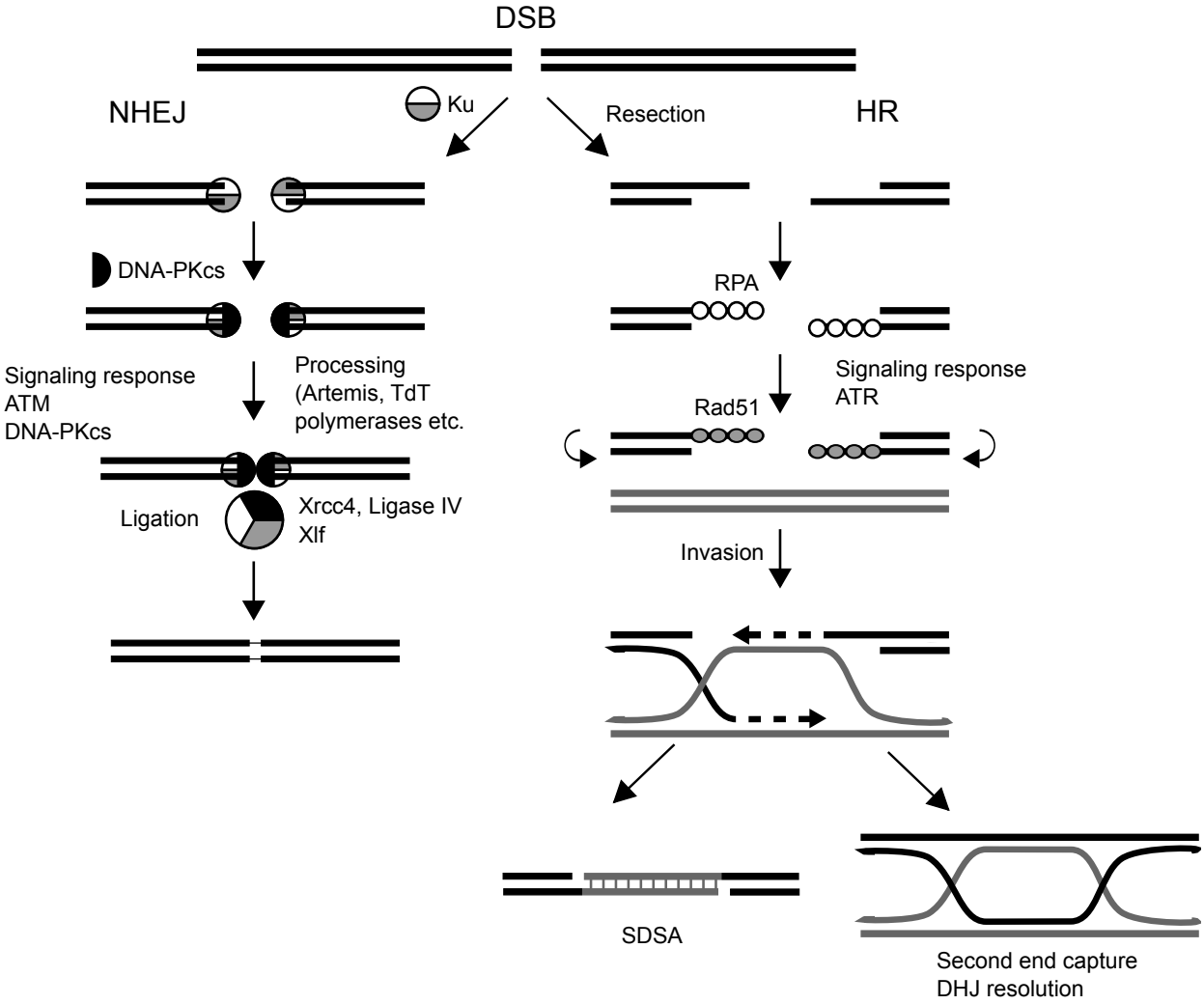

Figure 7.1: Double strand break repair pathways in mammalian cells. See text for details. Protein complexes are simplified and do not represent the exact stoichiometry or contacts.

veloping nervous system, as homozygous embryos display massive apoptosis in the developing nervous system. On a p53-deficient background, this apoptosis and the embryonic lethality is rescued and animals develop medulloblastomas and pro-B cell lymphomas (Frank *et al.*, 2000; Gao *et al.*, 2000). In the lymphoid lineage (in conditional knockouts or on a p53-deficient background), knockouts display the expected V(D)J recombination and class switch recombination defects.

Despite a strong radiosensitive phenotype in *Xlf*-deficient cells, the corresponding knockout mice do not show severe defects in V(D)J recombination, although they show some defects in class switch recombination later in development (Zha *et al.*, 2007; Li *et al.*, 2008). This distinguishes *Xlf* from the other 'core' NHEJ factors. What determines the requirement for *Xlf* in repair of DSBs, or rescues repair in its absence, remains unclear.

Some joining can still occur in the absence of NHEJ components. Cells lacking DNA-PKcs, Xrcc4 or Ligase IV can still repair a large fraction of IR-induced DSBs, albeit with slower kinetics compared to wild type cells (DiBiase *et al.*, 2000; Wang *et al.*, 2006). A low level of joining activity also occurs in V(D)J recombination on extrachromosomal substrates, and at double strand breaks induced by the I-*Sce*I nuclease (see below). Using these assays, the structure of the products can be examined by sequencing. In these mutant backgrounds, larger deletions are observed at the site of the break, often accompanied by apparently untemplated insertions of a few base pairs (Weinstock and Jasin, 2006; Guirouilh-Barbat *et al.*, 2007; Yan *et al.*, 2007). The deletions are often flanked by 'microhomology' of a few (2–6) base pairs, and are proposed to arise by annealing of these homologous sequences either side of the break. This has been proposed to provide synapsis, which may be lacking in cells deficient in core NHEJ components, and thus hold the ends together long enough for joining by another ligase, with deletion of the intervening sequence. The deletions and untemplated insertions may reflect multiple cycles of nucleolytic degradation and addition in the absence of repair. It has been suggested that this process may generate novel microhomology.

A likely candidate for the ligase in this so-called backup NHEJ (B-NHEJ) pathway is DNA Ligase III. Depletion of Ligase III from extracts from cells defective in the core NHEJ components further reduces joining activity (Wang *et al.*, 2005). Another factor implicated in the B-NHEJ pathway is poly(ADP-ribose) polymerase (PARP). There are several genes encoding PARPs in humans and mice, with PARP-1 and PARP-2 likely to represent the main activity in DNA repair (Amé *et al.*, 2004). Inhibiting PARP activity with small molecule inhibitors reduces end joining in Ku-deficient cells, but not in cells lacking Ligase IV (Wang *et al.*, 2006). This raises the possibility that PARP may act early in the pathway choice, at the same stage as Ku, and therefore inhibition has no effect in Ku-proficient cells.

NHEJ is active in all phases of the cell cycle. However, in late S phase and G2 phase, where a homologous template (the newly synthesised chromatid) is available, double strand breaks are more likely to be repaired by the process of homologous recombination (Rothkamm *et al.*, 2003).

Homologous recombination

Homologous recombination is the process of repairing DNA damage using sequence information from a homologue elsewhere in the DNA. Usually this is the allelic position on the sister chromatid; thus homologous recombination is only a major pathway of DNA repair in mammalian cells after replication has occurred, i.e. in S and G2 phases (Figure 7.1, Johnson and Jasin (2000)).

The process begins with 5′ to 3′ nucleolytic resection of the DNA flanking the double strand break. This resection produces 3′ single stranded DNA (ssDNA) overhangs. These are bound by a series of RPA protein monomers to form a protein-DNA filament. The presence of single stranded DNA activates the ATR (Ataxia telangiectasia related) kinase, which promotes downstream HR events and cell cycle arrest (Zou and Elledge, 2003). RPA is replaced by RAD51, a process dependent on BRCA2, which interacts functionally and physically with RAD51 (Scully *et al.*, 1997; Sharan *et al.*, 1997). This RAD51-ssDNA filament promotes homology searching and strand invasion on the homologous DNA. Synthesis to extend the invading strand allows use of sequence information from the homologue to fill any gaps and effect error-free repair. Both ends can be extended and ligated while still invading the homologue, producing a double Holliday junction (DHJ) which needs to be resolved, usually via BLM-TOP3α-RMI1/2. Alternatively, repair can be accomplished by extension of both ends templated by the homologue to create a compatible overlap, which can then anneal and be filled in and ligated. This is known as synthesis dependent strand annealing (SDSA). Both these pathways usually yield non-crossover products, although the DHJ pathway has the potential to produce crossovers if resolved by other enzymes. For further details, see Filippo *et al.* (2008).

7.1.3 Experimental induction of DNA double strand breaks

Random breaks

The most common technique to directly induce double strand breaks is to use ionising radiation (IR) or a radiomimetic drug such as bleomycin. IR produces double strand breaks, as well as single strand breaks and other complex damage, whereas drugs like bleomycin cause direct DNA breaks, which are often converted to double strand breaks (Steighner and Povirk, 1990). Such direct DNA damaging agents cause breaks throughout the cell cycle, and at many different loci. Studies using these methods usually look for repair *en masse*, either by using cellular survival as a proxy for successful repair or by looking at the extent of DNA breakage directly by electrophoresis techniques (Singh *et al.*, 1988). Individual breaks can be studied to an extent by looking at accumulation of DNA damage response proteins in nuclear foci, particularly phosphorylated histone H2AX (γ-H2AX), which are thought to form even in response to a single break (Rothkamm *et al.*, 2003). Irradiation of only part of the nucleus can also be accomplished using a laser, providing slightly more control over the induced damage (Kong *et al.*, 2009). Some cell cycle specificity can also be achieved by using drugs that cause single strand nicks, such as camptothecin. These are converted to double strand breaks when a replication fork passes—i.e. in S phase.

Locus-specific breaks

Experiments using the DNA damaging agents described above have provided many useful insights into the biology of DNA repair. However, in most cases the amount of damage caused is far in excess of any normal physiological setting and therefore the repair pathways may be unduly stretched. The main limitation of such assays is that as the locations of the breaks are not known, it is difficult to get information on the accuracy of the repair by sequencing repaired loci. This was the main incentive for the development of methods to experimentally induce single breaks at defined positions.

As mentioned above, B lymphocyte development involves induction of breaks at the IgH and IgL loci. These are programmed by recombination signal sequences (RSSs) in the DNA in the case of V(D)J recombination or switch (S) regions in the case of class switch recombination (CSR). T lymphocyte development also involves programmed breaks at the TCR loci. Although the breaks in these cases do occur in a defined region of the genome, the exact nucleotide position can vary. There are a number of possible RSS and S sites that can be cleaved, and in the case of S regions cleavage can occur at multiple positions within the S region. However, as the resulting joins can be cloned and sequenced, this has resulted in a number of important observations about end joining pathways—for example, that junctions often contain microhomology.

The most widely used mammalian experimental system to induce DSBs at a defined locus uses the I-*Sce*I restriction endonuclease. This has an 18 bp recognition site that is not present in the mouse or human genome. The recognition site is introduced as a transgene or on a plasmid, typically combined with suitable reporter genes. Transfecting cells with an I-*Sce*I expression plasmid results in cleavage at the recognition site (Rouet *et al.*, 1994). Several reporter constructs have been developed to allow different types of repair events to be recovered and measured. These have been used to discern the relative contributions of NHEJ and HR to repair (Liang *et al.*, 1998) and to investigate repair template choice (predominantly the sister chromatid, Johnson and Jasin (2000)), to name but two. The ability to program breaks at known loci by targeting I-*Sce*I sites into the genome has also been used for other purposes, such as the demonstration that double strand breaks at the targeted locus increase gene targeting frequency (Smih *et al.*, 1995).

The cleaved I-*Sce*I site has compatible 3′ four nucleotide overhangs. Precise ligation regenerates the cleavage site, and therefore the break may persist. This could result in a bias towards inaccurate repair in the recovered events. A recent study in which the Trex1 exonuclease was co-expressed with I-*Sce*I seems to support this theory (Bennardo *et al.*, 2009).

Another similar approach that has recently become available is the use of zinc finger nucleases. These can be designed to target specific sequences in the genome (via the zinc finger domains) and cause breaks by bringing a fusion partner, *Fok*I, into proximity of the targeted locus. The great attraction is that they do not require the introduction of an ectopic recognition site, and thus are being exploited as tools to create knockouts by simply cleaving and screening for inaccurate repair events. They have also been used to stimulate gene targeting and generate translocations as well as for the study of DSB repair (Porteus and Baltimore, 2003; Bibikova *et al.*, 2003; Brunet *et al.*, 2009). As for I-*Sce*I, there is a minor caveat about persistence of the break in this context, as accurate repair regenerates the cleavage

site.

7.1.4 Aims

In this chapter I describe experiments to determine whether or not the host DNA repair pathways are involved in repair of the PB-induced DSB. I found that the classical NHEJ pathway repairs all detectable breaks in the reporter system I describe, and therefore show that PB can be used to induce DSBs at known loci. I also argue that PB has several unique properties compared to other methods of DSB induction.

7.2 Results

7.2.1 Reporter cell lines with DNA repair deficiencies

Given that PB appears to leave compatible 5′ overhangs *in vitro* (Mitra *et al.*, 2008), and therefore does not require processing prior to ligation (although this is not ruled out), I decided to first investigate the ligation step of NHEJ as a likely host pathway to handle this lesion. I used two NHEJ-deficient ES cell lines —*Xrcc4*$^{-/-}$ and *Xlf*$^{\Delta/\Delta}$, both with homozygous mutations in components of the ligation complex (Zha *et al.*, 2007). These cell lines were a kind gift from Fred Alt and Shan Zha (Harvard). As noted above, *Xrcc4*$^{-/-}$ are effectively also Ligase IV deficient.

I already had a suitable reporter construct for excision, in the form of the TV28 targeting vector used to create the *Hprt*^{PB} reporter locus in Chapter 6 (Figure 7.2). The transposon is 667 bp from the nearest *Hprt* exon in this construct. Therefore, HAT selection can be used to isolate cells which have successfully repaired the PB-induced break. Even cells which repair the break inaccurately could be isolated, provided that transcription of *Hprt* is not disrupted. Finally, as the transposon contains the *puro*Δ*TK* gene, it is also possible to select cells that have lost the transposon and *not* regained *Hprt* function (6-TG selection). This should allow recovery of larger deletions that disrupt *Hprt* function (Table 7.1).

I used my transposon targeting vector (TV28) as before to insert the transposon into the *Hprt* locus in these cell lines, and also into JM8A3 wild type cells to use as a control. For JM8A3 and *Xrcc4*$^{-/-}$ cells, the targeting vector was in the TNN (*neo* expressing) orientation. Therefore I also transfected the targeted subclones with Cre to obtain the *puro*Δ*TK* expressing transposon required for FIAU selection. For the *Xlf* mutant targeting, I treated the targeting vector plasmid with recombinant Cre *in vitro* and transfected this linearised plasmid into cells as before. As the targeting efficiency was high in the previous experiment (at least 25%; Figure 6.4), I did not use 6TG selection to directly select for *Hprt* mutants.

Targeted clones were identified by PCR genotyping at the 5′ end relative to *Hprt* (Figure 7.3). As expected, the targeting efficiency was lower in the 129-derived cell lines that are not isogenic with the targeting vector (Figure 7.3 and Table 7.2). However, even under these suboptimal conditions, the targeting frequency was still at least 12% of G418 or Puro resistant subclones. Targeting was very efficient in the C57BL/6 cell line, in which almost 70% of G418-resistant clones were targeted—more than in the *Blm*-deficient background (see Figure 6.4). For all subsequent mobilisation experiments I used multiple targeted subclones as biological replicates. All clones used were checked to confirm correct targeting at the 3′ end and resistance to 10 μM 6-TG.

7.2.2 *Xrcc4* and *Xlf* are required for survival after transposition

I transfected 10^7 cells from each cell line with 15 μg of pCMV-hyPBase expression plasmid to mobilise the transposon. I plated a small fraction of transfected cells in M15 medium (non-selective) to determine the total colony forming units in the transfected cells. The remainder of the culture was plated at a higher density, and HAT selection begun 24 hours post transfection (Figure 7.4). As a negative control, I transfected cells with an equal amount of a GFP expression plasmid. These cells were selected as above, and in addition the transfection efficiency was determined in unselected cells by flow cytometry at 48 hours post transfection. Transfection efficiency (fraction of GFP-positive cells at 48 h) ranged from 37–52%.

There was a striking drop in the proportion of HAT resistant cells obtained for the mutant lines compared to the wild type (Figure 7.5). To compare the lines, I normalised the number of HAT resistant colonies for each subclone by plating and transfection efficiency. This analysis indicated that the mean survival after transposase selection and HAT selection in *Xrcc4* mutants is only 5% of the wild type value. For *Xlf* mutants, the surviving fraction was slightly higher at 11% of wild type. This demonstrates that reconstitution of a functional *Hprt* gene after transposon excision requires NHEJ.

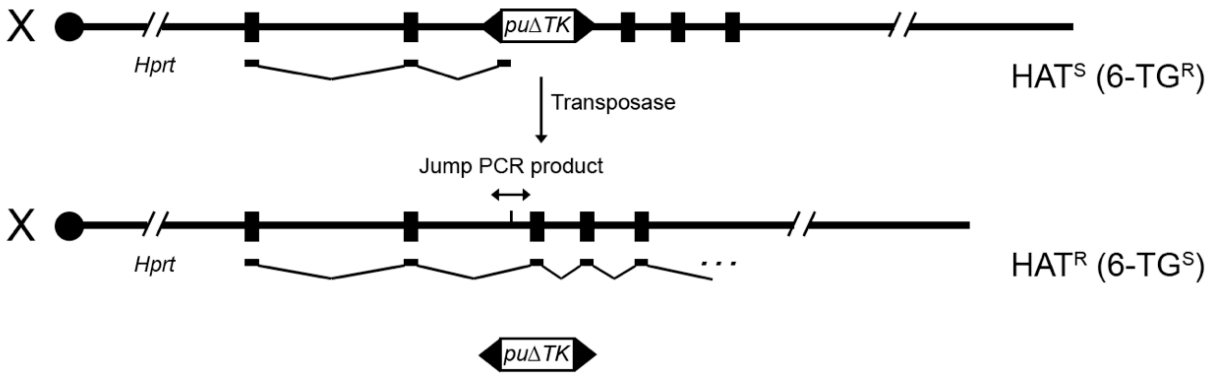

Figure 7.2: TV28 reporter locus for excision. See Chapter 6 for details

Event	Genotype	Resistance
Excision, successful repair (or small del)	*Hprt*$^+$	HAT
... with reintegration	*Hprt*$^+$, PB$^+$	HAT+Puro
Excision, no reintegration, large deletion	*Hprt*$^-$	FIAU+6-TG

Table 7.1: Transposition outcomes using the TV28 reporter locus. Selection schemes to detect transposition accompanied by successful repair (accurate or inaccurate)

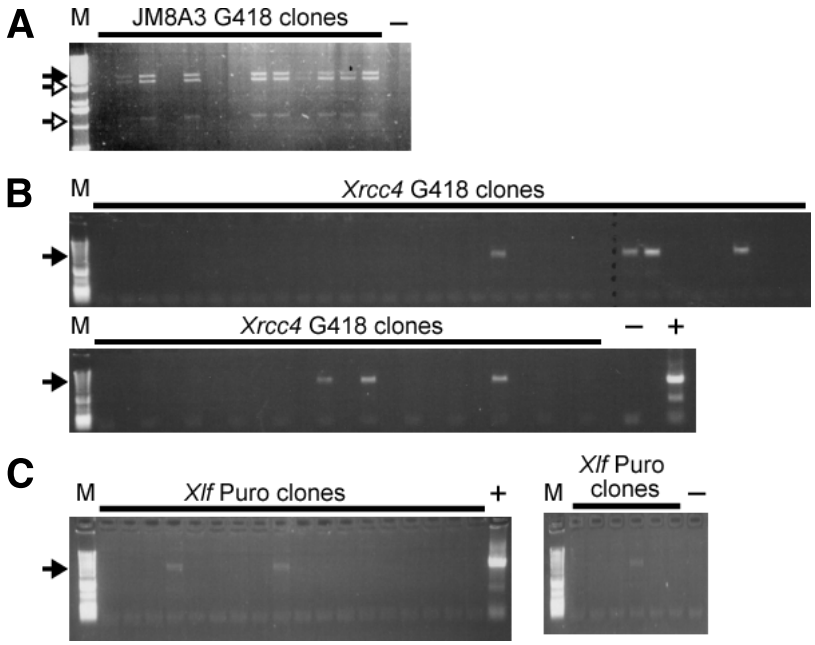

Figure 7.3: Targeting the *Hprt*^{PB} locus in NHEJ-deficient cells. PCR genotyping (as Figure 6.4) at the 5′ end of the targeting vector for A—JM8A3 (*neo* targeting vector) B—*Xrcc4*$^{-/-}$ (*neo* targeting vector) and C—*Xlf*$^{\Delta/\Delta}$ (*puro* targeting vector). The expected 4.2 kbp PCR product is shown with a filled arrow. Two smaller products (open arrows) are also amplified, although only in targeted clones, and probably arise due to one primer hybridising to a repetitive region of the PB repeat.

Cell line	Background	Genotyped	Targeted	Efficiency
JM8A3	C57BL/6N	13	9	69%
Xrcc4$^{-/-}$	129S7	60	7	12%
Xlf$^{\Delta/\Delta}$	129S7	24	3	13%

Table 7.2: Targeting efficiency in NHEJ-deficient cell lines

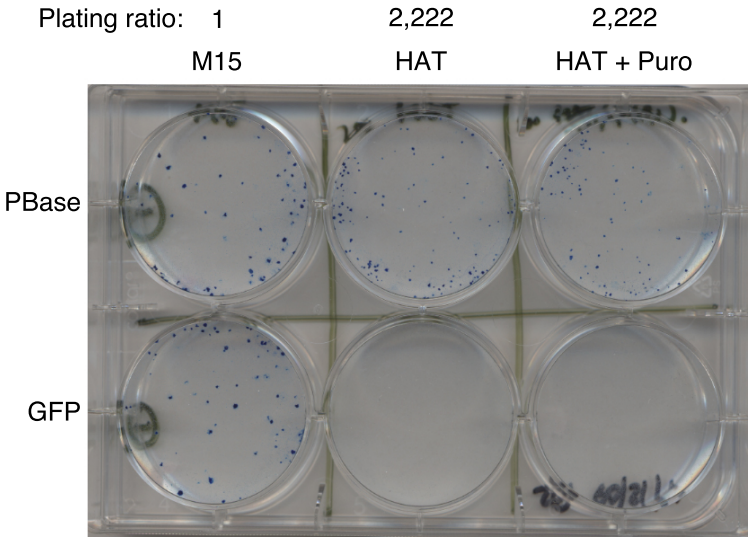

Figure 7.4: Example of transposition assay. *Xrcc4* reporter cells transfected with 15 μg of hyPBase or GFP expression plasmid are shown. M15—unselected cells to determine plating efficiency. 2,222 times as many cells are plated on the selected plates in this case. A much lower plating ratio (around 1:40) would be used for wild type cells.

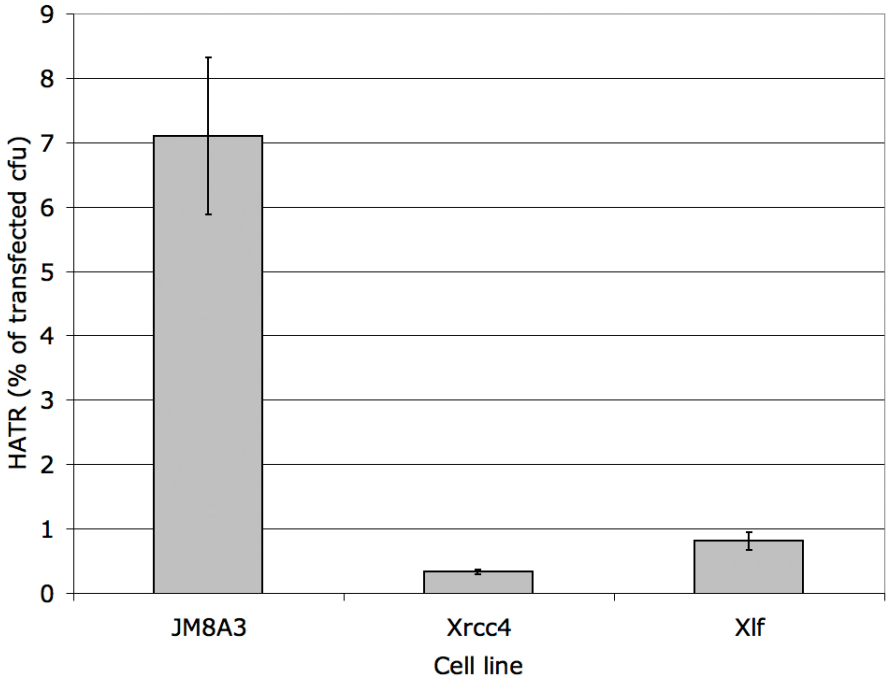

Figure 7.5: Survival in HAT medium following transfection of NHEJ reporter cell lines. The indicated wild type (JM8A3) or mutant cell lines were transfected with 15 μg pCMV-hyPBase as described in the text. The value plotted is corrected for transfection and plating efficiency. $n = 4, 6, 2$ respectively for JM8A3, *Xrcc4*$^{-/-}$, *Xlf*$^{\Delta/\Delta}$. Error bars show 95% confidence interval.

7.2.3 Mutations at the donor locus in *Xrcc4* mutants

Using primers that flank the donor site, I amplified a fragment from HAT resistant *Xrcc4*$^{-/-}$ subclones that had mobilised the transposon. PCR products from different clones, representing different transposition events, had clear size differences when separated on a 2% agarose gel (Figure 7.6A). The corresponding fragments from wild type cells were all of equal size, and sequencing revealed no mutations (Figure 7.6B and data not shown). When I sequenced the *Xrcc4*$^{-/-}$ PCR products, I found that all clones tested had deletions at the donor site, sometimes accompanied by a short insertion (Figure 7.7 and Table 7.3). The deletions without insertions were often flanked by 2–4 bp microhomologies. Some events (defined by the extent of deletion on each side) were recurrent, particularly those without insertions and with microhomology flanking the deletion. Events with insertions were more variable with respect to the extent of deletion.

As microhomologies are short by definition, and usually less than 5 bp in length, it is difficult to be sure that they do not simply occur by chance, and thus whether they are really characteristic of the repair. A formula has been developed to address this, although it assumes a random sequence of a given GC content, as it was developed to analyse non-site specific breaks (Roth *et al.*, 1985). The sequence surrounding the break in this case is always the same, and furthermore is not random, as there is some vector sequence present close to the break from the cloning procedure (see Chapter 6). Therefore a better approach would be to consider microhomology use in the context of this particular sequence. To address this, I generated a distribution of the microhomology that would be expected by chance. Taking the sequence surrounding the breakpoint, I modelled a random resection of up to 20 nt at each end to determine how often microhomologies of 1–4 nt would be encountered if resection was randomly terminated. Plotting these with the experimental data shows a clear increase of junction microhomology of two or more nucleotides in the sequenced junctions compared to that expected by chance (Figure 7.8).

In other cases the deletion was accompanied by an insertion. In most cases these were short and not obviously derived from surrounding sequence. I only isolated a single event that could be classified as accurate with respect to the TTAA site, but this had a single base pair deletion immediately downstream, so could also have resulted from a deletion and reinsertion of nucleotides. These data indicate that *Xrcc4* is required for accurate repair of all PB induced breaks.

In most cases where a deletion flanking the donor locus was accompanied by an insertion, this was short and not uniquely mappable to the genome. These could arise from untemplated nucleotide additions by polymerase enzymes during end processing. It is possible that such additions could generate new microhomologies, which can then be used to anneal the two ends to each other. However, in three cases I observed larger mutations with a clear structure. Two of these had a duplication of sequence from both sides of the break. However, the arrangement of the sequences from either side of the break was shuffled (Figure 7.9 and Figure 7.10A,B). One possible way to generate this structure might be a duplication after repair is complete, although the event shown in Figure 7.10B is not perfectly duplicated.

Another event with a large insertion turned out to have the terminal 245 bp of the PB5 end of the transposon remaining in the locus, which was then joined to downstream genomic sequence. Two nucleotides of microhomology were present at the site of joining (Figure 7.11). One possible explanation for this is that only one end of the transposon was cleaved, followed by extensive degradation and rejoining. However, as the genomic end adjacent to PB5 was not degraded, a more likely possibility may be that this event occurred in late S/G2 phase and involved some homology-directed repair from the unjumped sister chromatid, followed by microhomology-mediated joining to the other free end.

7.2.4 Low frequency of mutations at the donor locus in *Xlf* mutants

I also sequenced the donor locus in 44 subclones from the *Xlf* mutant cells (Figure 7.12 and Table 7.4). In contrast to the *Xrcc4* mutants, most (37/44) repair events were precise in these cells. This is in broad agreement with the results of an extrachromosomal V(D)J recombination assay in these cells (Zha *et al.*, 2007). Three clones had deletions with clear flanking microhomologies, and two events were also recovered with structured insertions—one with a 72 bp repetitive insertion, and one with a duplication of 16 bp of sequence from one side of the break.

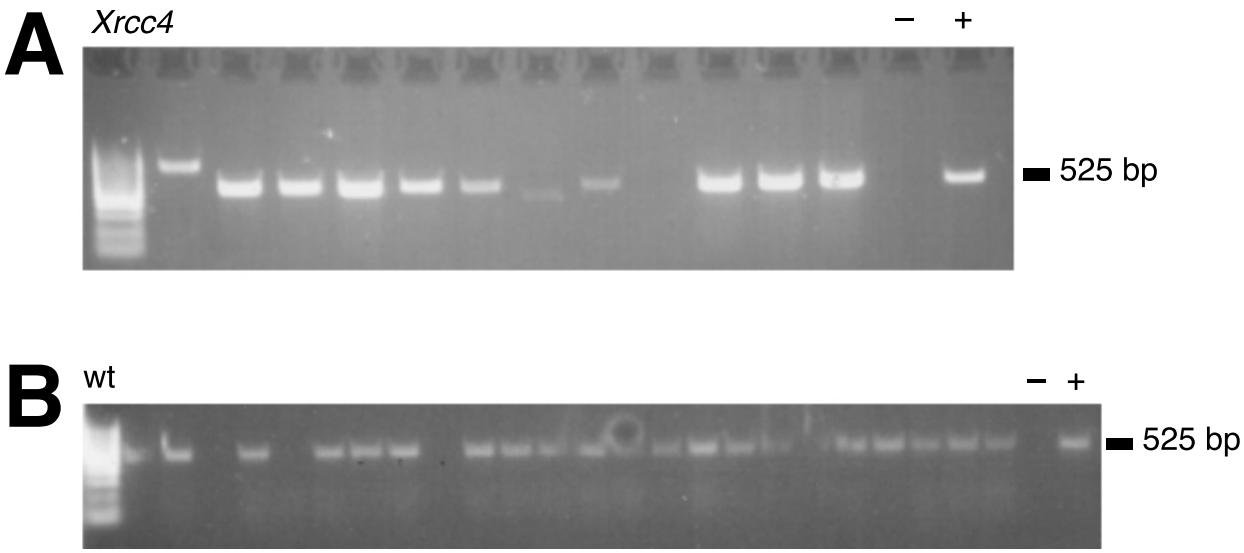

Figure 7.6: PCR amplification of donor locus after transposition. A—Products from *Xrcc4* mutants are different sizes, indicating insertions and/or deletions have occurred. B—All products from wild type cells are normal. +: Template DNA from known mobilised LGN cells, –: No template DNA added.

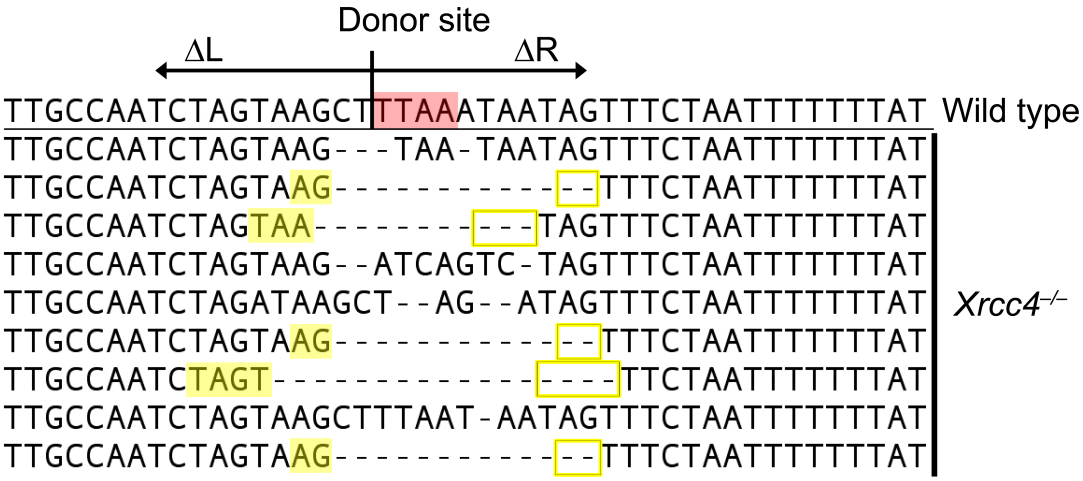

Figure 7.7: Examples of mutations at the donor site in *Xrcc4* mutants. The cleavage point on the strand shown is indicated by a vertical bar. ΔL,R show the deleted base pairs as summarised in Table 7.3. Microhomologies flanking the deleted sequence are highlighted in yellow on the left of the deletion, the position of the corresponding identical sequence on the right, which is deleted, is boxed (refer to the aligned accurate repair sequence on the top line).

# clones	ΔL	Insertion	ΔR	μ-hom
1	0	AG	4	
1	0	AG	5	
1	0		6	T
1	0	AG	7	
1	0		8	
1	0		9	T
1	0	AACA	10	
1	0		16	CT
1	0	TTAA	5**	
1	1	19 bp*	5	
1	1	AAACTAA	5	
1	1	30 bp*	7	
1	2	275 bp*	0	
2	2	T	3	
1	2		5	
1	2	T	7	
1	2	ATCAGTC	8	
7	2		11	AG
1	2	TAATAACTGATT	105	
1	3		5	
4	3		8	TAA
1	3		11	
2	5		12	TAGT
1	7	A	15	
1	10		9	AAT
36				

Table 7.3: Sequencing of the repair site in *Xrcc4* mutants. For the wild type sequence see Figure 7.7. ΔL—number of base pairs deleted on the 'left' side (5′ with respect to *Hprt*), ΔR—size of deletion on 'right' side, μhom—microhomology observed flanking deletion. Insertions marked with * are shown in more detail in Figure 7.9. ** Could also be classified as accurate, with a 1 bp deletion.

# clones	ΔL	Insertion	ΔR	μ-hom
37	0		0	
1	0		3	
1	0	TAGATTAGTTTCTAAT	8	
1	0		9	T
1	3	$(CCCTAA)_{12}$	5	TAA
1	3	*	8	TAA
1	4		5	TA
1	5		12	TAGT
44				

Table 7.4: Mutations at donor locus in *Xlf* mutants. * Duplication of sequence adjacent to the breakpoint as shown in Figure 7.10C. The insertion shown in row 3 was not uniquely mappable.

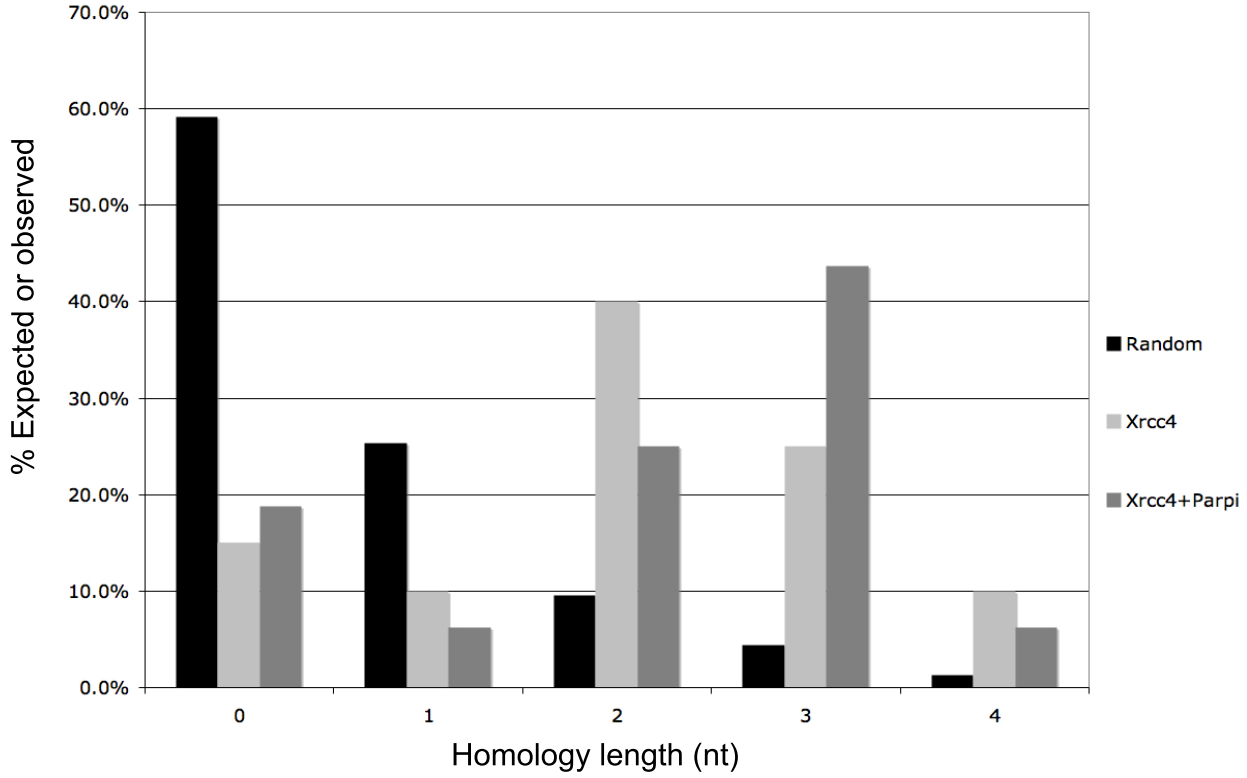

Figure 7.8: Expected and observed use of microhomology of the indicated lengths at repair sites. Expected value (black bars) is calculated based on a random resection of the break (up to 20 nt). The observed distribution in *Xrcc4* mutants is plotted in light grey. Dark grey bars—*Xrcc4* mutants treated with PARP inhibitor as described in text. Repair events that also contained an insertion are omitted; the inserted nucleotides may have generated novel microhomology, but this cannot be concluded from the final sequence.

	Xrcc4	*Xlf*
Accurate	1	37
Deletion (w/μhom)	21 (17)	4 (3)
Deletion + insertion	11	1
Deletion + insertion with clear structure:		
Duplication of sequence from both sides	2	
Truncated transposon (275bp)	1	
One-sided duplication		1
Short repeats (CCCTAA)x12		1
	36	44

Figure 7.9: Structure of insertions at excision site in NHEJ mutants. The transposon is shown as a dark arrow. Not to scale.

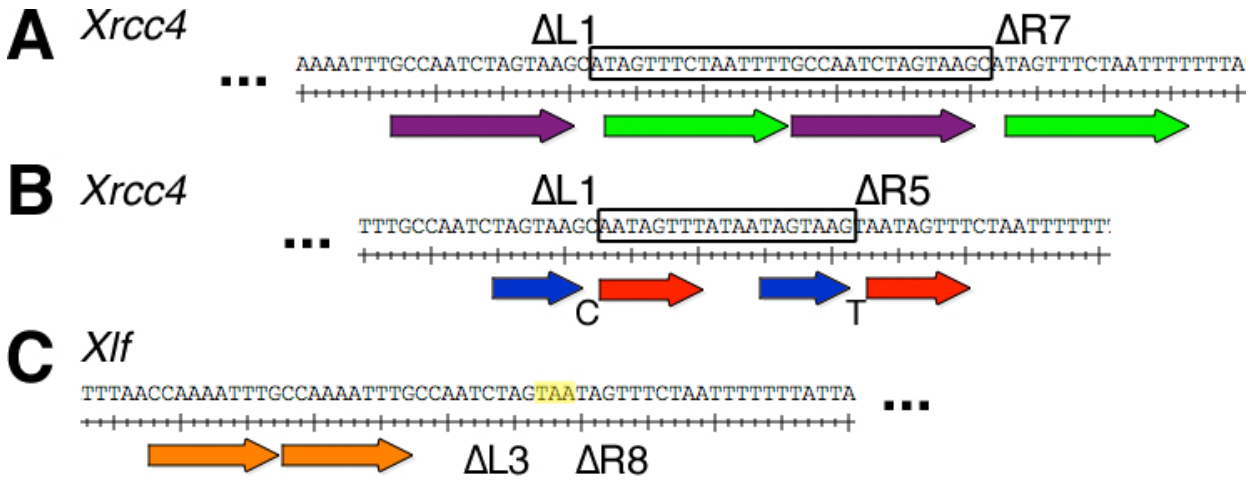

Figure 7.10: Sequence of insertions with clear structure. A, B—duplications from *Xrcc4* mutants. The duplication in A is perfect while the sequence in B has differences in the nucleotides separating the individual and pairs of repeats. The inserted sequence is shown in a box. C—Sequence from *Xlf* mutant showing a tandem duplication upstream of the excision site. There is a deletion at the excision site (with associated TAA microhomology highlighted in yellow). ΔL, ΔR give sizes of deletion observed either side of the break, as Figure 7.7.

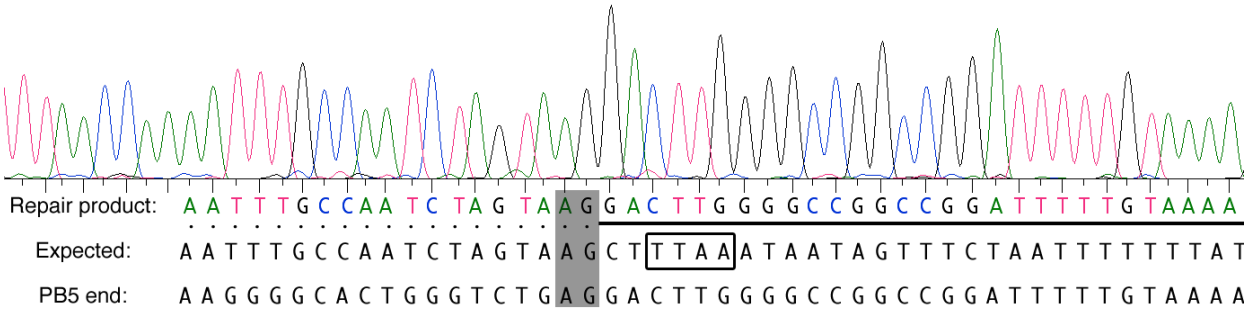

Figure 7.11: Junction sequence of a repair event retaining part of the transposon, isolated from the *Xrcc4* mutant. Sequence and chromatogram of the PCR product sequence is shown, aligned with the expected sequence in the case of accurate repair, and the proximal PB5 end sequence. Potential microhomology (AG) at the site of joining is highlighted; the excision site is shown in a box in the expected sequence.

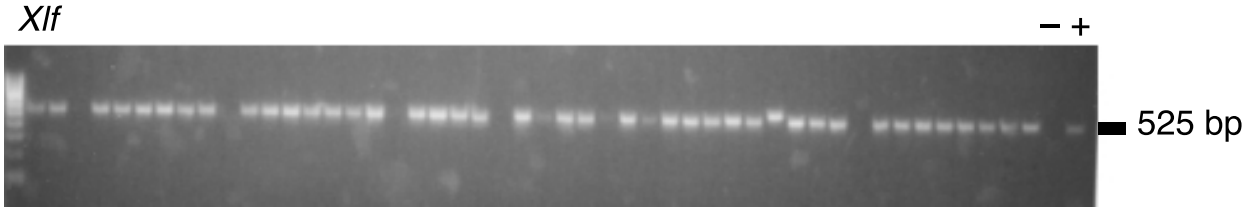

Figure 7.12: PCR amplification of donor locus from *Xlf* mutants, as Figure 7.6.

7.2.5 No evidence for larger deletions related to transposition in *Xrcc4* mutants

As many repair products from *Xrcc4* mutants had deletions, it is possible that the decrease in HAT resistant clones is due to large deletions that destroy *Hprt* function. To test this, I repeated the transfection of transposase and subsequently cultured the cells for three days without selection. I then replated the culture in selective medium containing 6-TG and FIAU at low density (1×10^5 cells per 90 mm plate). This low density is necessary to avoid cross-killing of *Hprt* negative cells by nearby *Hprt* positive cells that can metabolise 6-TG.

Colonies were obtained on the selective plates in this experiment even without transfection of the PBase plasmid (Figure 7.13). These may arise from a high mutation rate or silencing affecting the *Puro-ΔTK* gene in the *Xrcc4* mutant cells. However, there was no obvious increase in the number of colonies in cells transfected with the transposase plasmid. This suggests that the 'missing' transposition events that are not recovered under HAT selection in the *Xrcc4* mutant cells do not arise from large deletions that destroy *Hprt*.

7.2.6 PARP inhibition does not affect repair in the absence of *Xrcc4*

An increased use of microhomology during end joining has been reported for cells defective in several of the components of the core NHEJ pathway. This has been termed, variously, backup end joining (B-NHEJ) or alternative end joining (Alt- or A-NHEJ). However, as the factors responsible have not been conclusively identified, it remains to be seen whether describing alt-NHEJ as a distinct pathway is accurate. One obvious requirement is a ligase. There are only two other ligases apart from Ligase IV in mammals: Ligase I and Ligase III. Biochemical experiments indicate that Ligase III is probably responsible for joining in the absence of Ligase IV (and also in the absence of XRCC4). Ligase III is an essential gene in mammalian cells (Puebla-Osorio *et al.*, 2006), and no specific inhibitors are currently available. This precludes further analysis using my system. Another factor implicated in the alt-NHEJ process is PARP activity. Inhibition of PARP in Ku deficient cells resulted in a further reduction in end joining, although this was not seen in Ligase IV deficient cells (Wang *et al.*, 2006). As highly potent and specific PARP inhibitors are available, I decided to see if these would affect end joining in my *Xrcc4*-deficient system. I treated reporter cells for two hours prior to transfection with 10 μM KU-0058948 (A gift from S.P. Jackson and KuDOS/AstraZeneca, (Farmer *et al.*, 2005)), then carried out electroporations as above. The cells were maintained in medium with the inhibitor for 24 hours, then selected in HAT medium without inhibitor. Treatment with the inhibitor affected cell viability, but HAT resistant colonies could still be obtained (Figure 7.14A, B). Taking the lower viability into account, neither excision nor reintegration appeared to be affected in cells treated with the inhibitor (Figure 7.14C). I amplified and sequenced 21 donor sites in total. The mutation spectrum appeared similar to the untreated *Xrcc4*-deficient cells, with no significant change in deletion length, types of mutation observed or microhomology use (Table 7.5 and Figures 7.8 and 7.16). There was a slightly higher proportion of microhomology-mediated deletions relative to deletions accompanied by short insertions, but this was not statistically significant ($P = 0.13$, one-sided binomial test). Recurrent events were not observed in the presence of the inhibitor (Table 7.5). This could reflect a role of PARP in regulating end processing, leading to a higher diversity of joining events, but more events would need to be analysed to investigate this. These minor alterations in the types of repair event aside, PARP activity does not seem to be required for repair in the absence of *Xrcc4*. This is in agreement with the results obtained in Ligase IV deficient cells (Wang *et al.*, 2006). These data support the conclusion that PARP acts upstream of Xrcc4-Ligase IV in end-joining pathway choice.

7.2.7 Excision and reintegration are not affected by inhibitors of PARP, ATM or DNA-PKcs in wild type cells

The recent development of potent and specific inhibitors of DNA repair enzymes for potential therapeutic use has provided a new set of tools for the study of DNA repair (Jackson, 2009). The PB system for precise induction of DSBs complements these drugs well, as a variety of perturbations can be studied using the same reporter cell line and the same break. I used my wild type reporter cell line with some of these small molecule inhibitors to address several questions.

First, although the experiments described above demonstrate that the host NHEJ machinery is involved in repair of the transposon excision site, whether the host DNA repair machinery is involved in reintegration *in vivo* remains to be determined. The

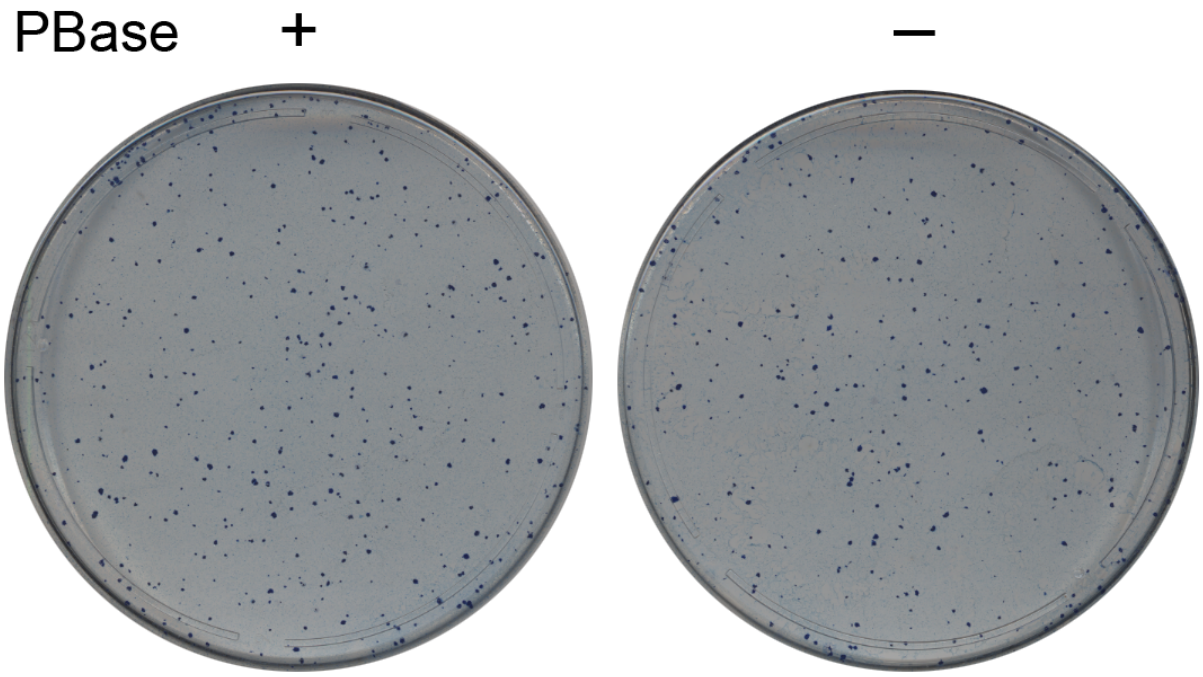

Figure 7.13: FIAU+6-TG selection to detect large deletions. *Xrcc4*$^{-/-}$ cells were transfected with hyPBase (+) or GFP (–) expression plasmids, and replated in FIAU+6-TG after three days. There is a high background, but no obvious PBase-dependent increase.

# clones	ΔL	Insertion	ΔR	μ-hom
1	0		0	
1	0	CT	4	
1	0	TATAATTA	4	
1	0		7	
1	0	TTTATTAG	13	
1	1		3	TTA
2	1		6	
4	1		10	TTA
1	1		21	A
1	4		10	TA
1	5		8	CT
1	5	TACTAATTGAATTG(AAAAATTAGA)AGCT	8	
1	6		11	AC
1	12		17	ATT
1	18		1	TAAA
1	20		10	TA
1	42		7	AGC
21				

Table 7.5: Mutations at the site of repair in *Xrcc4* cells treated with a PARP inhibitor. The bracketed portion of one insertion is mappable, to a sequence just downstream of the break on the reverse strand; otherwise the insertions are not uniquely mappable.

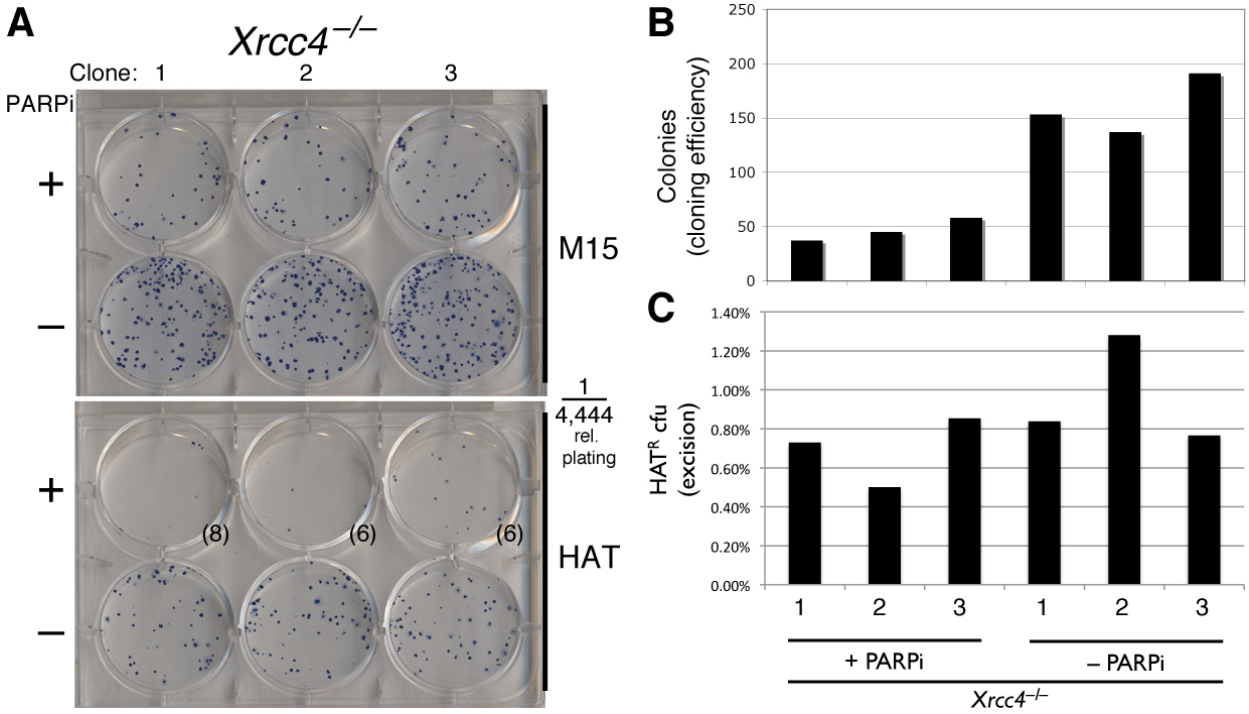

Figure 7.14: Results of transposition in *Xrcc4* mutant cells treated with PARP inhibitor. A—A low frequency of HAT resistant colonies are obtained, showing that excision is not completely abolished. PARPi treatment also reduces the number of colonies on the untransfected plate (M15). Numbers in brackets for plates with few colonies show number of colonies that were picked for analysis. B—Colony counts of unselected colonies. C—Frequency of HAT resistant cells post-transposition (corrected for cloning efficiency) is not affected by PARPi treatment. Results are from three independent subclones.

Type	*Xrcc4*$^{-/-}$	*Xrcc4*$^{-/-}$ + PARPi	*Xlf*$^{\Delta/\Delta}$	w.t.
Normal	1	1	37	17
μhom del	17	13	3	0
other del	3	3	1	0
del + ins $<$ 5nt	9	1	0	0
del + ins $>$ 5nt	6	3	3	0
Total analysed	36	21	44	17

Table 7.6: Summary of types of event observed in different mutants

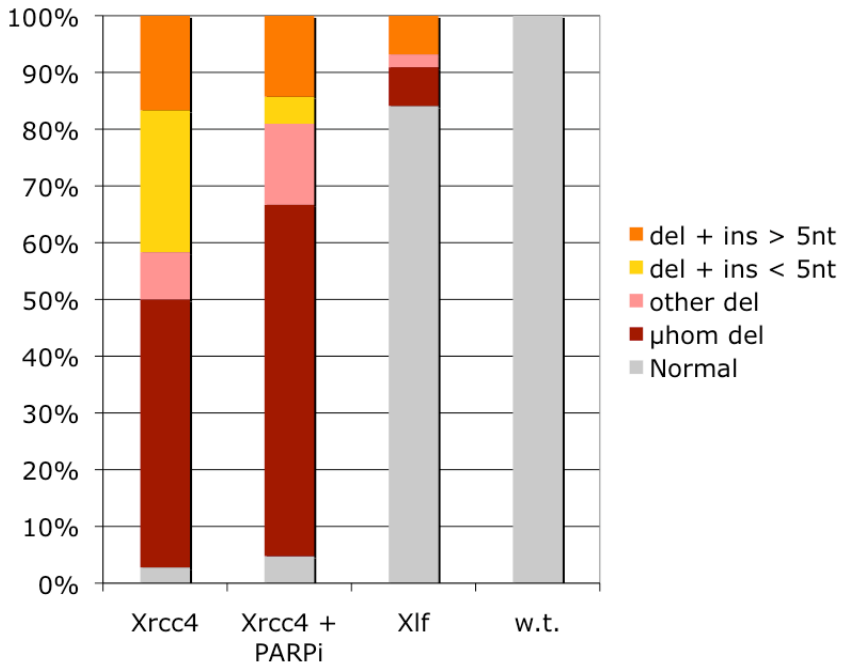

Figure 7.15: Graph showing frequency of repair event classes in different mutants

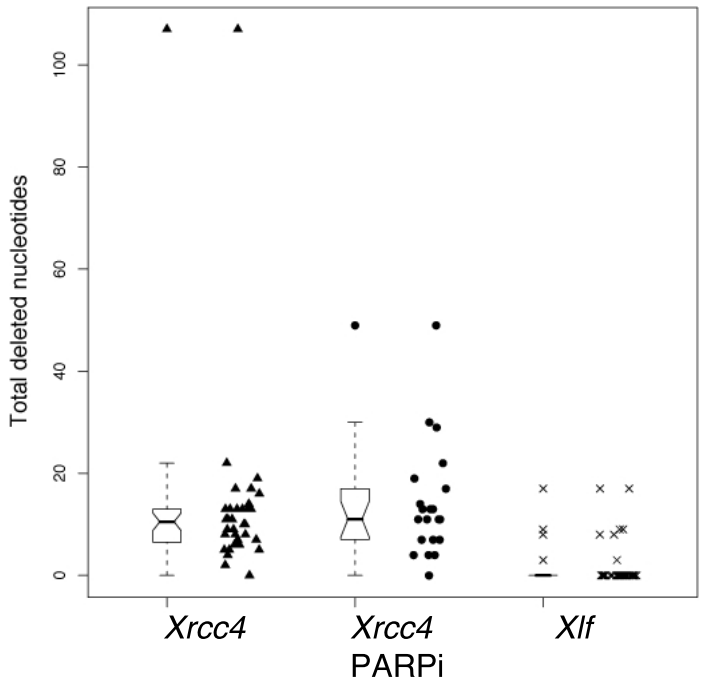

Figure 7.16: Distribution of total deletion size (ΔL + ΔR) at repair site in NHEJ mutants.

transposase is sufficient to join at least one strand *in vitro* (Mitra *et al.*, 2008). As the excised transposon is likely to be capped by hairpins, these could be dependent on DNA-PKcs for processing by analogy with coding ends in V(D)J recombination. I treated cells with the DNA-PKcs inhibitor NU-7441 (Tocris Bioscience, used at 1 μM, 2 h pre-transfection, 24 h post-transfection) and carried out the transposition assay as above. Both HAT and HAT+Puro resistant clones were obtained, at frequencies similar to untreated cells. This indicates that reintegration is not dependent on DNA-PKcs (Figure 7.17), and suggests that the observation that the transposase is sufficient to join excised transposons to the target site *in vitro* applies *in vivo*.

I also tested inhibitors of ATM and PARP using this system. ATM is required for the repair for some DSBs, but what determines whether or not it is required for a particular break is unclear. Using the ATM inhibitor KU-55933 (Tocris Bioscience, used at 10 μM with pretreatment as for NU-7441, above), I determined that ATM is not required for the repair of the PB-induced break in my reporter cells (Figure 7.17).

I also checked the effect of PARP inhibitors, and obtained similar results to the *Xrcc4* mutants above—i.e. a decrease in cell survival that was not PB-dependent, and no clear change in the excision or reintegration frequency (Figure 7.17).

7.2.8 Homologous recombination repair of PB-induced breaks

The cell lines described in this chapter do not allow repair of the break by HR to be assessed directly. The most likely template for HR is the sister chromatid. In the reporter cells, the sister chromatid will also contain a transposon—therefore repair of the break by gene conversion will restore the transposon in the *Hprt* locus and not result in HAT resistance. Even if the transposons on both sister chromatids are mobilised, there is no way to tell sister chromatids apart at the sequence level. Previous methods for detection of HR using the sister chromatid have used reporters with direct repeats, where crossing over between the distal repeat unit on one chromatid with the proximal on the other results in three copies of the repeat on one of the resulting chromatids (Johnson and Jasin, 2000). HR using a homologous chromosome is not possible in my system, as the reporter is on the X chromosome.

7.3 Discussion

7.3.1 Requirement for host repair pathways in repair of PB-induced breaks

Experiments using the reporter cell lines described in this chapter show that *Xrcc4* and *Xlf*, components of the NHEJ pathway, are required for recovery of HAT-resistant clones after transposition. There are two possible reasons for the failure to recover HAT-resistant clones, assuming the same number of excision events from the *Hprt* locus. One explanation is that NHEJ mutant cells cannot repair the break, and subsequently die or enter senescence and do not form a colony. Alternatively, the break could be repaired imprecisely and in the process destroy *Hprt* function, for example by causing a large deletion.

However, although the system is able to detect deletions of at least 100 bp (Figure 7.16), almost all deletions are distributed in the 1–20 bp interval. If this size distribution is in fact bimodal, with a second peak of undetected large deletions, this could explain the results. It is difficult to envisage a mechanism for such a distribution based on known DNA repair mutant phenotypes, and the results of FIAU+6-TG selection (Figure 7.13) suggest that there are not a large number of cells bearing large deletions affecting *Hprt*.

Another alternative to death would be restoration of a transposon at *Hprt* from the sister chromatid by HR, if excision occurs in S or G2 phase. These would also not be picked up by the HAT selection system, nor by FIAU+6-TG selection. One potential improvement to the reporter system would be to select for the excision independently of *Hprt* function. This could be accomplished by using a gene trap transposon at a known locus where a gene is not trapped. Mobilisation of this transposon could be selected for by selection for reintegration events that do trap a gene. The original locus could then be examined by PCR or Southern blotting, allowing the full range of mutations to be detected.

It should be noted that although this system allows a single repair event to be studied at the donor locus, there may be multiple breaks elsewhere in the cell if the transposon reintegrates and jumps again. This may affect the sensitivity measurements, as there may be more than one break in some cells (if the transposon jumps again before repair of the previous break), or breaks induced persistently over the expression period of the transposase. Little is known about the kinetics of PB transposition, so the effect is hard to predict.

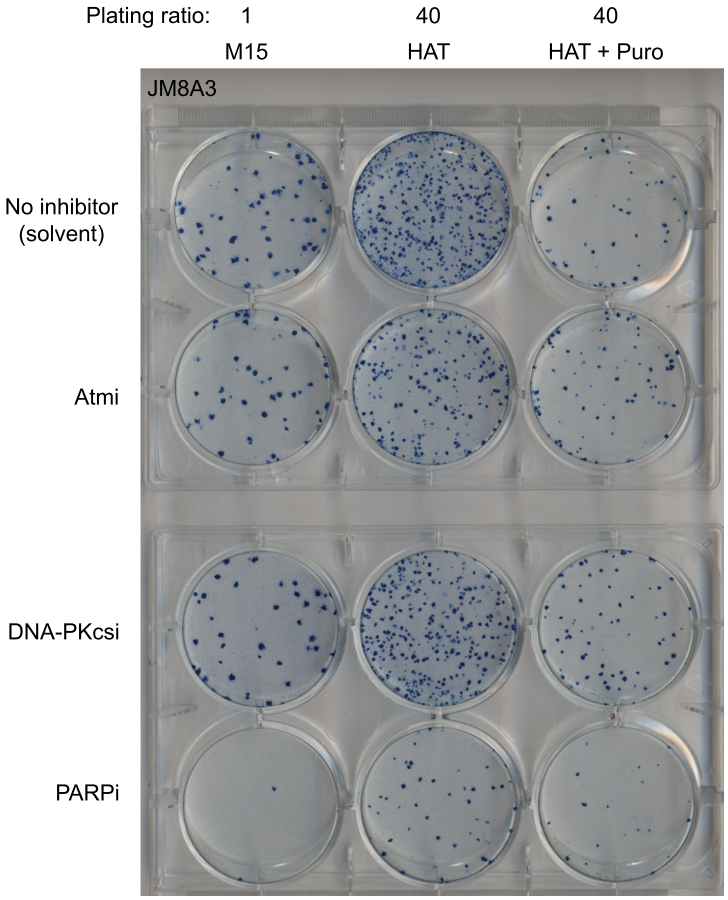

Figure 7.17: Transposition assay in wild type cells treated with ATM, DNA-PKcs and PARP inhibitors as indicated.

It would be interesting to investigate whether there is any involvement of HR in repair of the transposon. Gene targeting is dependent on components of the HR pathway (Essers *et al.*, 1997; de Wind *et al.*, 1995), and double strand breaks introduced by I-*Sce*I or zinc finger nucleases stimulate gene targeting at the locus of the break (Smih *et al.*, 1995). Therefore, if PB induced breaks are indeed processed in the same way as an endogenous break, they should also stimulate gene targeting at the donor locus. This could be investigated by attempting to stimulate targeting at the *Hprt* locus in the reporter cell line by transfection with PBase.

Potential effect of genetic background

The two mutant cell lines used are from the 129S7 genetic background, while the wild type cells used for comparison are C57BL/6N. Therefore any differences could potentially arise from different genetic backgrounds. Similar transposition assays have been carried out in 129S6 and 129S6×C57BL/6J genetic backgrounds by colleagues (Wang *et al.* (2008); Liang *et al.* (2009) and K. Yusa, unpublished) with similar excision efficiencies obtained. No differences in DNA repair have been documented between the genetic backgrounds used, and as the *Xrcc4* mutant defect is so severe and produces a known phenotype with respect to the structure of the recovered products, it is unlikely that genetic background alone could be responsible for the difference. However to formally prove this, the experiment should be repeated in TC1 wild type cells [the 129S7 cell line that the NHEJ mutants were derived from], or in complemented cells expressing *Xrcc4* or *Xlf* transgenes as appropriate.

7.3.2 Differential requirement for *Xrcc4* and *Xlf* at PB-induced breaks

The two NHEJ mutant cell lines studied *are* derived from the same parental cell line, and can be directly compared. It had been previously noted that $Xlf^{\Delta/\Delta}$ cells had a less severe radiosensitivity compared to $Xrcc4^{-/-}$ cells. Western blotting and overexpression experiments have confirmed that the *Xlf* allele is a genuine null (Li *et al.*, 2008). This implies that *Xlf* is dispensable for repair of some IR-induced lesions. IR causes different types of break, often with complex structures, at different loci as well as causing multiple lesions per cell.

My results show that the difference in IR sensitivity between these two mutant lines extends to the single break caused by PB transposition. The constant nature and location of the break in my system raises the question of what the basis is for this differential requirement for the two NHEJ factors. One possible explanation may be a difference in NHEJ at different stages of the cell cycle; this is something that could be addressed using the G1-specific PBase-CDT1 fusion protein described in the previous chapter.

7.3.3 DNA repair requirements in V(D)J recombination and PB transposition

The mechanism of PB excision is similar to V(D)J recombination, in that hairpin ends are produced that then need to be resolved before joining. In V(D)J recombination, these hairpin ends (coding ends) require DNA-PKcs and Artemis for repair. Structurally these are analogous to the PB transposon ends (Figure 7.18). I therefore asked whether PB reintegration, as opposed to excision, had similar requirements. As I did not have DNA-PKcs or Artemis deficient ES cells available, I used a recently developed DNA-PKcs inhibitor instead. The experiment did not show an effect (Figure 7.17). It should be noted that DNA-PKcs inhibitors or kinase-dead DNA-PKcs mutants do not always reproduce the phenotype of DNA-PKcs knockouts, suggesting that DNA-PKcs also performs a structural role in DSB repair that is separable from its kinase activity. However, as the transposase is sufficient for hairpin resolution in a defined *in vitro* system, I favour the explanation that this extends to the *in vivo* situation. Thus the host DNA repair pathway is only responsible for repair of the excision site and not involved in reintegration.

This is perhaps reasonable considered in the light of evolution: DNA repair pathways are efficient and highly conserved across vertebrates; therefore there is probably no need for the transposon itself to handle excision site repair, and no selective pressure for this function. The DNA repair machinery does suppress translocations and is likely to fuse free transposon ends to form a circle, as with V(D)J recombination signal ends, so the transposase needs to take control of the reintegration. Interestingly, both the RAG1/2 recombinase and SB transposase appear to interact with Ku, which is proposed to channel repair of the excision site into the NHEJ pathway. It would be interesting to see if PB has a similar association.

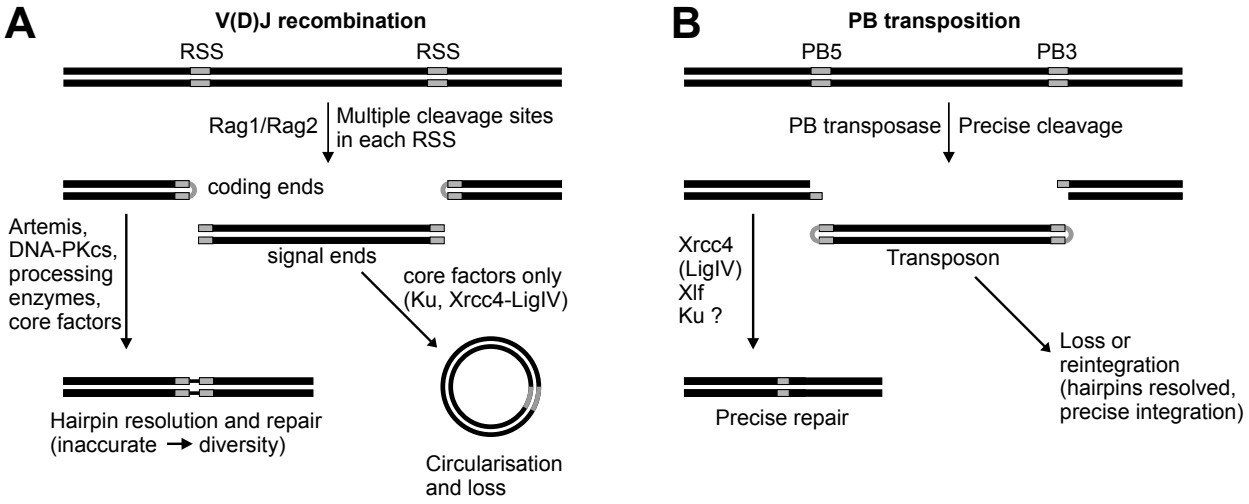

Figure 7.18: Requirements of NHEJ factors in V(D)J recombination and PB transposition. The structure of the different DNA ends formed and subsequent products are shown (not to scale). A—V(D)J recombination, B—PB transposition

7.3.4 DNA repair requirements in SB transposition

The requirements for various DNA repair factors in SB transposition have previously been investigated (Izsvák *et al.*, 2004). It should be emphasised that while SB and PB are often thought of as similar in terms of their role as mouse genetic tools, they belong to distinct transposon families with different mechanisms. However, as both cause double strand breaks, there is likely to be some similarity in the requirement for host repair pathways. Izsvák *et al.* used an integration assay in Chinese hamster ovary (CHO) cells with various DNA repair defects. Using this system, the authors concluded that SB transposition required Ku80, XRCC4, ATM (in some cases) and DNA-PKcs, although not DNA-PKcs kinase activity. Although transposition in this case was from a plasmid, junctions could be recovered by PCR and sequenced. In all the mutant lines for which junctions were recovered, there were deletions flanking the excision site, and for ATM and Ku80 mutants these appeared to be flanked by microhomology. Interestingly the authors of this study were unable to recover junctions from XRCC4 mutants, whereas I could readily amplify PCR products.

There are several differences between the assays used that could explain this. First, the breaks left by the two transposons may not be dealt with in the same way. SB leaves incompatible overhangs, and as mentioned above, the transposase may directly interact with Ku to affect repair. Second, the break in the SB assay is on a plasmid, while in my system, the break is genomic and thus presumably occurs in an appropriate chromatin context. Transiently transfected plasmids may not reflect the situation for genomic breaks. Finally, my system incorporates selection for repair and subcloning prior to PCR and sequencing, which may make it easier to isolate rare repair events, e.g. those in *Xrcc4* mutants. A further advantage is that the distribution of accurate/inaccurate repair events in the products is not affected by bias in PCR, gel cutting or subcloning.

7.3.5 Advantages of PB for programming double strand breaks

The experiments described here suggest an alternative use of PB: as a system to create locus-specific DSBs in cells and study their repair. PB has a number of features that distinguish it from other enzymes used for this purpose (Table 7.7). Using PB, cell lines with single copy insertions at known random positions can be easily generated (see e.g. Figure 5.2). With a transposon carrying suitable negative selectable markers to detect excision, DSBs at a variety of different loci could be studied. It would be interesting to use such a method to determine if breaks at some loci require Atm activity for repair—in my system, the break is at an expressed locus. IR-induced breaks that require Atm for repair are associated with heterochromatin, suggesting that knowing the exact locus of a break and its

dependence on Atm would be useful in investigating this further (Goodarzi *et al.*, 2008). This could be done in many different cell types without the need for gene targeting or extensive screening for single copy transgenics to introduce enzyme recognition sites for I-*Sce*I. One potential caveat would be that PB may have a preference for euchromatin (see Chapter 3), so the SB transposon, which has different epigenetic preferences (Wang *et al.*, 2008), may be a better option for such a study.

One unique aspect of PB is that the excision site cannot be recleaved after transposition. This is in contrast to the endonucleases where accurate repair reconstitutes the recognition site, which can then be recleaved. Thus I-*Sce*I-induced breaks, for example, are persistently recleaved until they are repaired inaccurately. This could lead to a bias towards inaccurate repair events in the observed products, which does not reflect the actual accuracy of the process. In my system, each HAT-resistant colony represents a single repair event that can be easily subcloned and analysed. These attributes of PB make it a useful tool for making careful measurements of repair accuracy under different circumstances, and provide a method for simple analysis of mutations at the sequence level. It would be particularly interesting to use cell cycle specific transposase enzymes, as described in Chapter 6, to induce and study cell cycle specific breaks.

Enzyme	Rec. site	End structure	Persistant?	Transgenic req?
I-*Sce*I	18 bp	3′ 4 nt	Yes	Yes
Zn-finger-*Fok*I	customisable	5′ 4 nt	Yes	No
PBase	4 bp + Tn	5′ 4 nt	No	No

Table 7.7: Comparison of different site specific nuclease systems for causing experimental DSBs